

**Supplementary Information For:**  
**Electrochemically Identified Ultrathin Water Oxidation Catalyst in Neutral  
pH solution Containing Ni<sup>2+</sup> and its Combination with Photoelectrode**

Sung Ki Cho<sup>†,\*</sup> and Jinho Chang<sup>‡</sup>

<sup>†</sup>*Department of Energy and Chemical Engineering, Kumoh National Institute of Technology,*

*61 Daehak-ro, Gumi-si, Gyeongsangbuk-do 730-701, Republic of Korea, \*E-mail:*

*chosk@kumoh.ac.kr*

<sup>‡</sup>*Department of Chemistry and Center for NanoBio Applied Technology, Sungshin Women's  
University, 55, Dobong-ro, 76ga-gil Gangbuk-gu, Seoul 142-732, Republic of Korea.*

<b>Table of Content</b>	<b>Page</b>
1. Electrochemical and spectroscopic analyses on “Ni-Pi” (Figure S1)	2-3
2. Cyclic voltammograms of various electrodes in PB solution containing Ni <sup>2+</sup> (Figure S2)	4
3. GC measurements of oxygen evolved from water-oxidation catalyzed by Ni <sup>2+</sup> (Figure S3)	5
4. EQCM responses in PB solution containing Ni <sup>2+</sup> (Figure S4)	6-7
5. The Ni Pourbaix diagram at 298 K (25°C) in water (Figure S5)	8
6. CVs of Au UME (10 μm dia.) in PB solution containing Ni <sup>2+</sup> (Figure S6)	9
7. CVs of FTO in the various buffer solutions containing Ni <sup>2+</sup> (Figure S7)	10
8. CVs and chronoamperograms in the solution containing 0.1 M reactant (Figure S8)	11
9. Numerical Simulation of Catalytic Reaction of Ni <sup>2+</sup> ion in PB solution (Figure S9)	12
10. Photoresponses of BiVO <sub>4</sub> with Ni <sup>2+</sup> for the oxidation of sulfite and water (Figure S10)	14
11. IPCE for the photoelectrochemical water oxidation on BiVO <sub>4</sub> with Ni <sup>2+</sup> (Figure S11)	15
12. CVs of FTO in PB solution containing Ni <sup>2+</sup> in comparison with Co <sup>2+</sup> (Figure S12)	16
13. Rough estimation of turnover frequency of Ni <sup>2+</sup> -WOC	17

# 1. Electrochemical and spectroscopic analyses on “Ni-Pi”

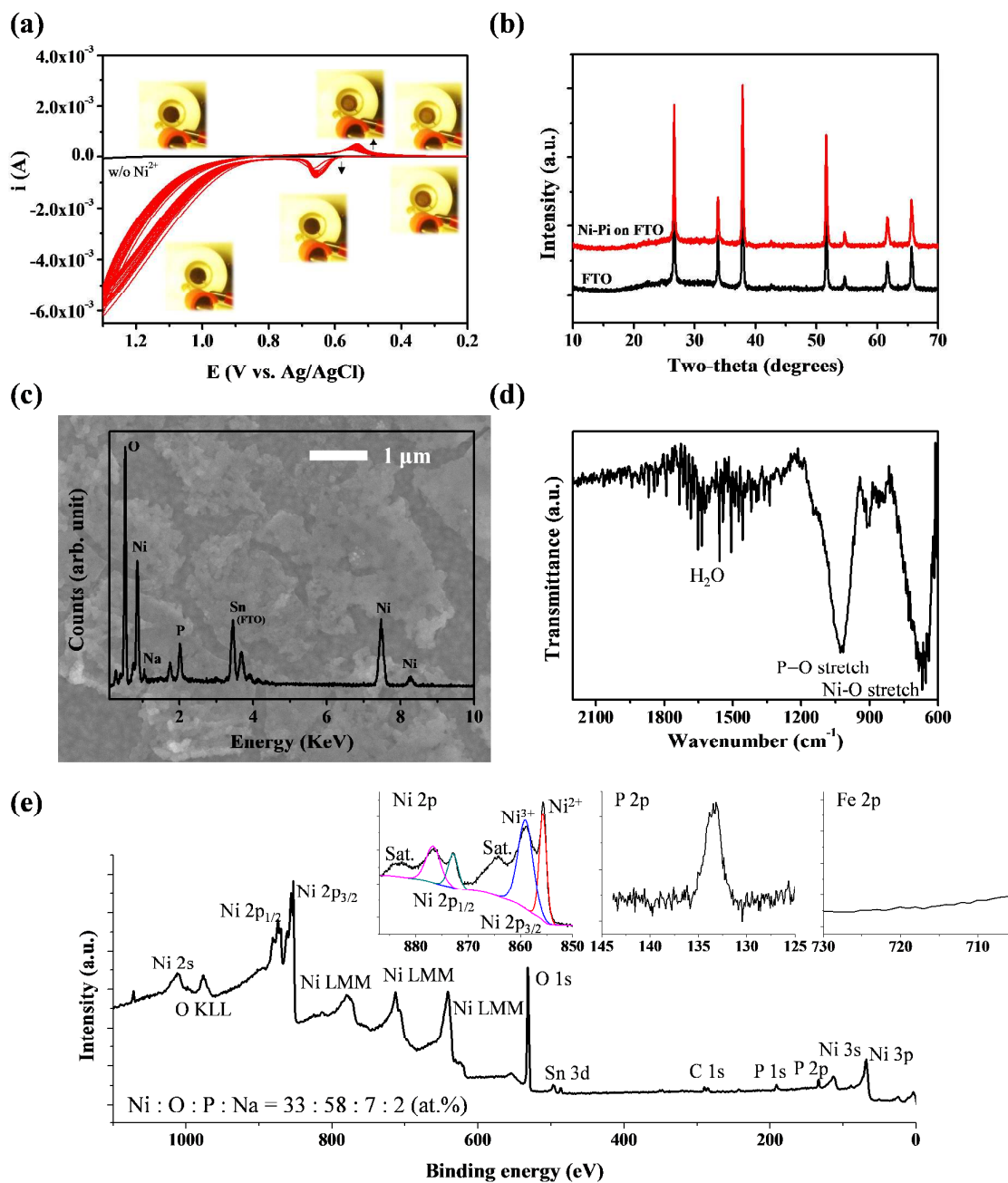


Figure S1. (a) Cyclic voltammograms of FTO (1 cm<sup>2</sup>) with multiple cycling in the phosphate solution (0.1 M HPO<sub>4</sub><sup>2-</sup>, 0.1 M H<sub>2</sub>PO<sub>4</sub><sup>-</sup>, and 0.2 M NaOH, pH 11.5) solution containing 2 mM Ni<sup>2+</sup>. Inset images are the photograph of film at each potential region, which indicates the

electrochromatic behavior of “Ni-Pi” film on FTO ( $1 \text{ cm}^2$ ). (b) X-ray diffractometry (X-MAX, Rigaku, Cu  $K\alpha$  radiation source), (c) Scanning electron microscopy-energy dispersive spectroscopy (JSM-6500F, JEOL), (d) attenuated total reflectance (ATR) Fourier transform infrared (FT-IR) spectrometry (Vertex 80V, Bruker), and (e) X-ray photoelectron spectroscopy (K-Alpha, ThermoFisher, monochromatic Al X-ray source) analyses results of “Ni-Pi” electrodeposited at 1.5 V (vs. Ag/AgCl) for 3000 s in the phosphate solution (0.1 M  $\text{HPO}_4^{2-}$ , 0.1 M  $\text{H}_2\text{PO}_4^-$ , and 0.2 M NaOH, pH 11.5) solution containing 2 mM  $\text{Ni}^{2+}$ . The composition ratio of Ni to buffer in “Ni-Pi” is similar with that in “Ni-Bi” (Mircea Dincă, Yogesh Surendranath, and Daniel G. Nocera, Nickel-borate oxygen-evolving catalyst that functions under benign conditions, PNAS, 2010, 107 (23), 10337–10341.). For ATR-IR measurement, “Ni-Pi” electrodeposited on a FTO substrate was loaded and clamped on a single reflectance diamond crystal ATR accessory (PLATINUM ATR, Bruker), which was mounted on the FT-IR spectrometer. The spectrum of a pristine FTO substrate was used as the reference spectrum.

2. CVs of various electrodes in PB solution containing  $\text{Ni}^{2+}$

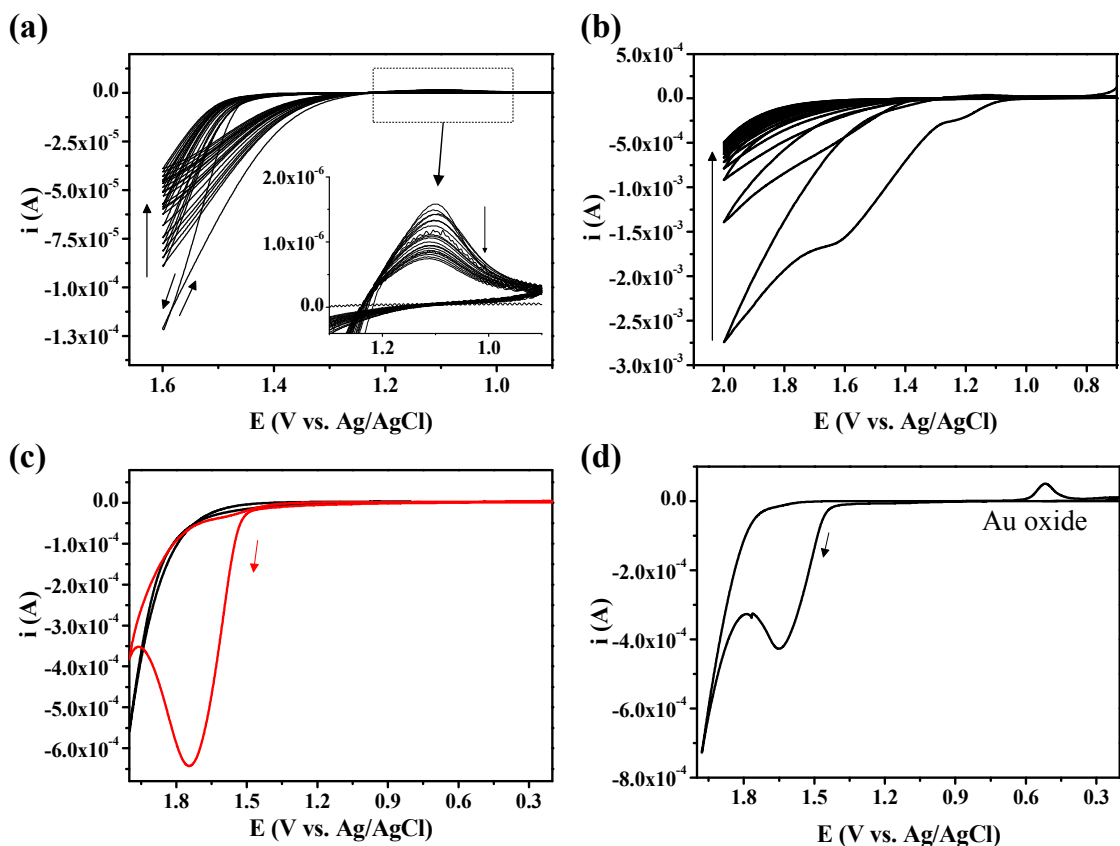


Figure S2. (a) Multi-cyclic voltammograms (scan rate 20 mV/s) of (a) FTO ( $0.0314 \text{ cm}^2$ ) in pH 6.8 phosphate buffer ( $\text{HPO}_4^{2-} : \text{H}_2\text{PO}_4^- = 1:1$ ) solution containing  $2 \text{ mM Ni}^{2+}$ , and (b) "Ni-Pi" on FTO ( $1 \text{ cm}^2$ ) in pH 6.8 Ni-free phosphate buffer. "Ni-Pi" film was formed by applying 1.5 V (vs. Ag/AgCl) for 2000 s in the phosphate solution ( $0.1 \text{ M HPO}_4^{2-}$ ,  $0.1 \text{ M H}_2\text{PO}_4^-$ , and  $0.2 \text{ M NaOH}$ , pH 11.5) solution containing  $2 \text{ mM Ni}^{2+}$ . Cyclic voltammograms of (c) GC ( $0.071 \text{ cm}^2$ ) and (d) Au ( $0.0314 \text{ cm}^2$ ) disk electrodes in pH 7 phosphate buffer ( $0.1 \text{ M HPO}_4^{2-} / 0.1 \text{ M H}_2\text{PO}_4^-$ ) solution containing  $2 \text{ mM Ni}^{2+}$  (scan rate: 50 mV/s)

3. Gas chromatography (GC) measurements of oxygen evolved from water-oxidation catalyzed by  $\text{Ni}^{2+}$

Experimental details. A gas-tight single compartment electrochemical cell composed of a carbon working electrode ( $0.42 \text{ cm}^2$ ), a Pt wire counter electrode, a Ag/AgCl reference electrode, and a pH 6.8 phosphate buffer ( $0.1 \text{ M HPO}_4^{2-}/0.1 \text{ M H}_2\text{PO}_4^-$ ) electrolyte was connected to a GC system (Agilent 7890A) equipped with a thermal conductivity detector (TCD), where the evolved gas on the working electrode was directly delivered to the sampling loop of a gas chromatography in real-time through the outlet of the glass cell at the top of the working electrode. The evolved gas on the positively polarized carbon working electrode ( $1.7 \text{ V vs. Ag/AgCl}$ ) was analyzed every three minutes during the electrolysis. During the electrolysis, the electrolyte was stirred vigorously with the stir bar.

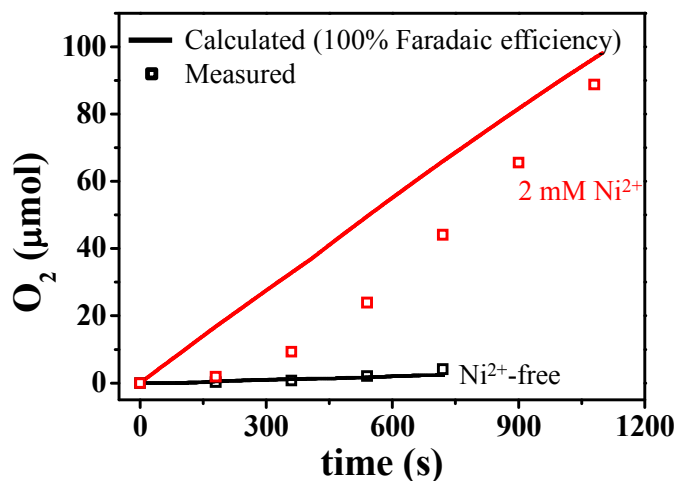


Figure S3.  $\text{O}_2$  amount measured by GC (empty square symbol) and theoretical amount (solid line), assuming a Faradic efficiency of 100% with and without  $\text{Ni}^{2+}$  in a pH 6.8 phosphate buffer ( $\text{HPO}_4^{2-} : \text{H}_2\text{PO}_4^- = 1:1$ ).  $1.7 \text{ V vs. Ag/AgCl}$  was applied on carbon paper electrode ( $4.2 \text{ cm}^2$ ).

#### 4. EQCM responses in PB solution containing $\text{Ni}^{2+}$

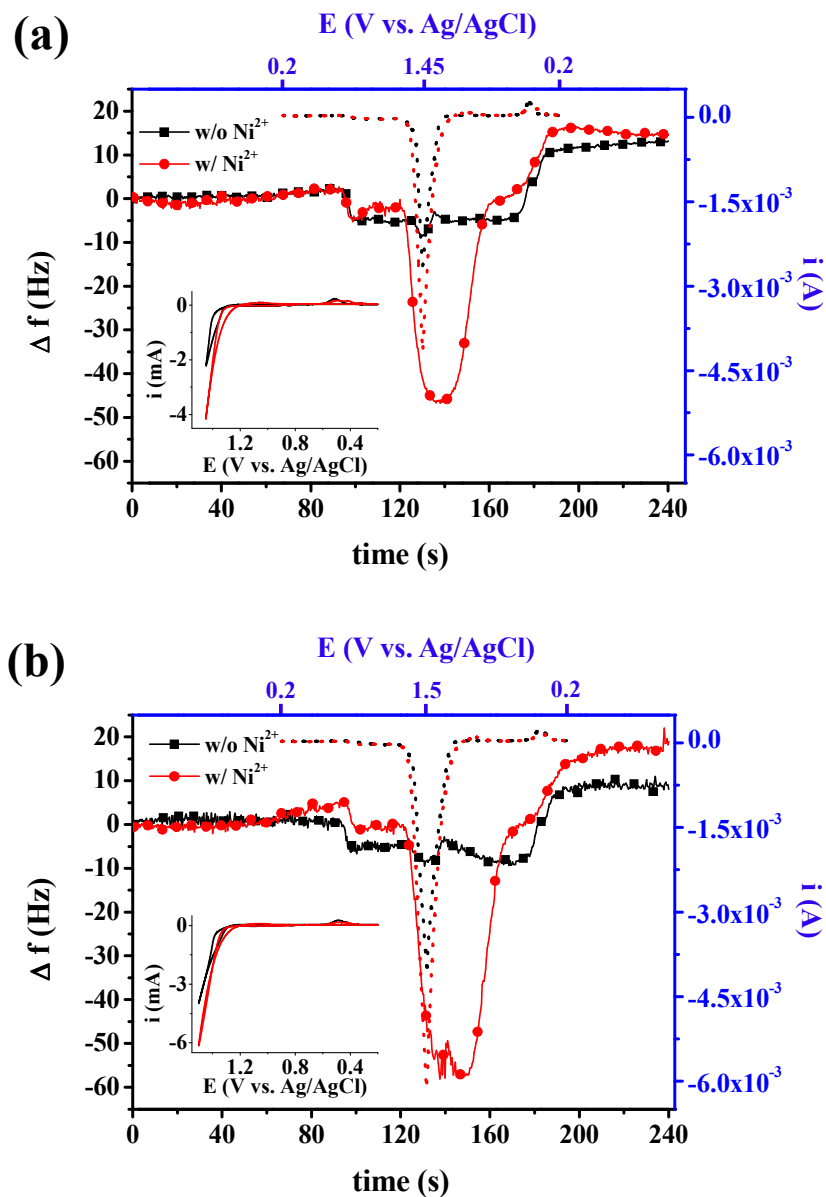


Figure S4. The frequency change of Au-coated quartz crystal ( $1.0 \text{ cm}^2$ ) in EQCM during cyclic voltammetry in pH 6.8 phosphate buffer ( $\text{HPO}_4^{2-} : \text{H}_2\text{PO}_4^- = 1:1$ ) solution containing 2 mM  $\text{Ni}^{2+}$ , with the potential cycling (a) between 0.2 V (vs. Ag/AgCl) and 1.45 V or (b)

between 0.2 V and 1.5 V. A change of frequency ( $\Delta f$  in Hz) can be converted to a mass change ( $\Delta m$  in  $\text{g}/\text{cm}^2$ ) by the equation;

$$\Delta f = -C_f \times \Delta m$$

where  $C_f$  is the sensitivity factor for the crystal (i.e.  $56.6 \text{ Hz}/\mu\text{g}\cdot\text{cm}^2$  for a 5MHz AT-cut quartz crystal at room temperature), and the change in the mass of the electrode herein was  $8.46 \times 10^{-7} \text{ g}/\text{cm}^2$  and  $1.10 \times 10^{-6} \text{ g}/\text{cm}^2$ , respectively.

5. The Ni Pourbaix diagram at 298 K (25°C) in water (H<sub>2</sub>O)

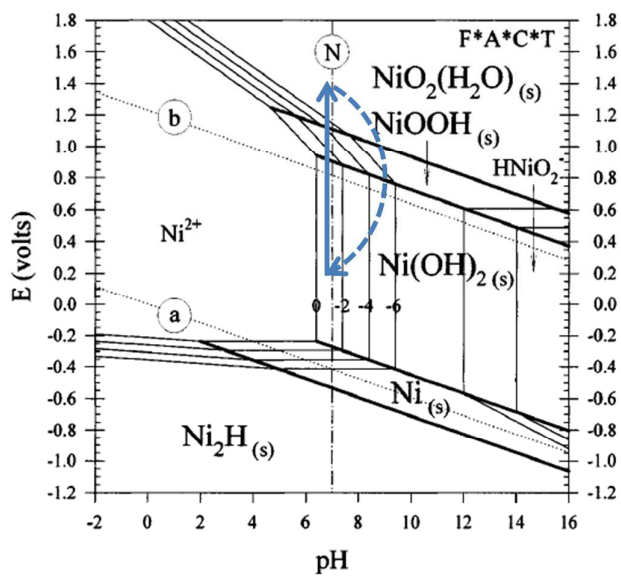


Figure S5. The Ni Pourbaix diagram at 298 K (25°C) in water (H<sub>2</sub>O). The concentration of Ni<sup>2+</sup> ranges from 1 to 10<sup>-6</sup> M, and the blue arrow indicates change in the potential during cyclic voltammetry. (Ref. FACT EpH-Web, <http://www.crct.polymtl.ca/ephweb.php>)



6. CVs of Au UME (10  $\mu\text{m}$  dia.) in PB solution containing  $\text{Ni}^{2+}$

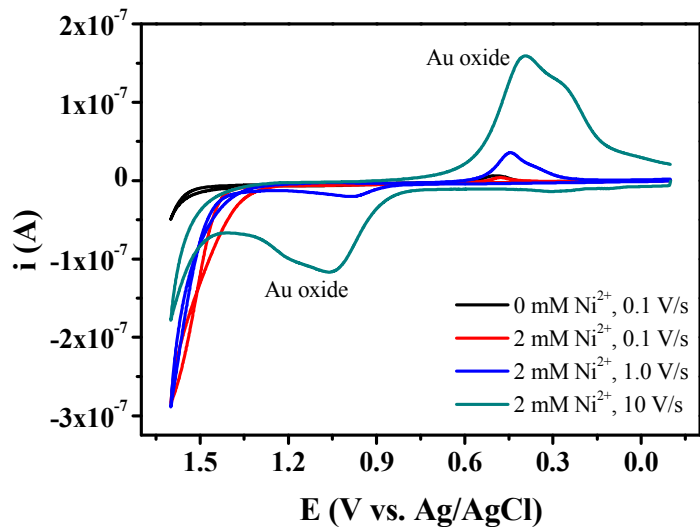


Figure S6. Cyclic voltammograms of Au ultramicroelectrode (10  $\mu\text{m}$  dia.) in pH 6.8 phosphate buffer (0.1 M  $\text{HPO}_4^{2-}$ /0.1 M  $\text{H}_2\text{PO}_4^-$ ) solution containing  $\text{Ni}^{2+}$  with different scan rate. The distinct redox peaks were associated with the oxidation of Au surface and following reduction (J. C. Hoogvliet and W. P. van Bennekom, Gold thin-film electrodes: an EQCM study of the influence of chromium and titanium adhesion layers on the response, *Electrochim. Acta*, 47 (2001), 599-611.). Au UME was used in order to rule out the increase in the capacitance with higher scan rate.

7. CVs of FTO in the various buffer solutions containing  $\text{Ni}^{2+}$

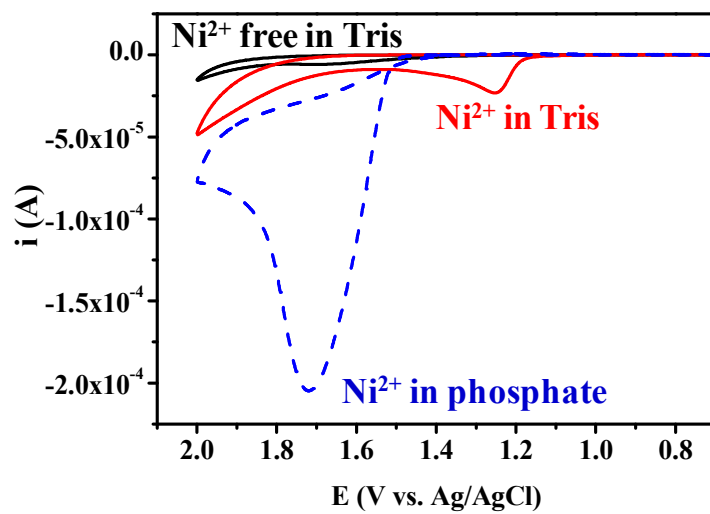


Figure S7. Cyclic voltammogram of FTO ( $0.0314 \text{ cm}^2$ ) in pH 6.8 phosphate buffer (0.1 M  $\text{HPO}_4^{2-}/0.1 \text{ M H}_2\text{PO}_4^-$ ) solution or pH 7 Tris buffer (0.1 M) containing  $\text{Ni}^{2+}$  (scan rate: 20 mV/s)

8. CVs and chronoamperograms in the solution containing 0.1 M reactant

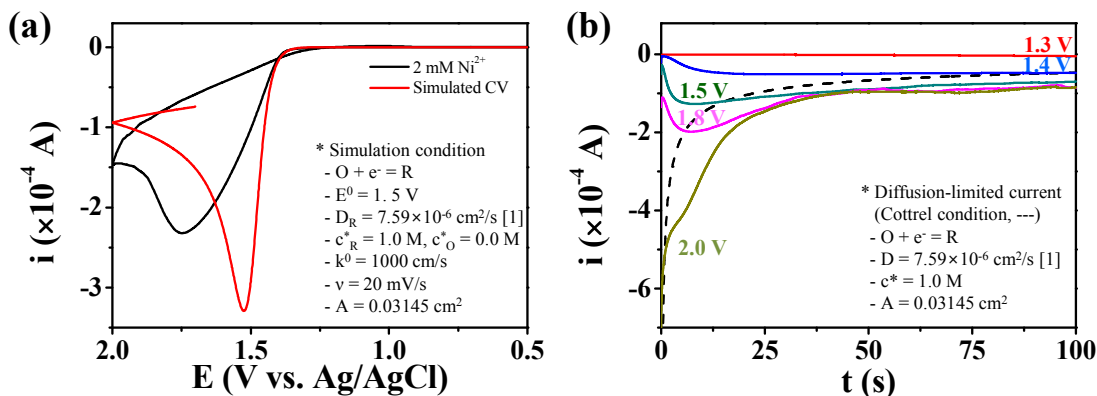
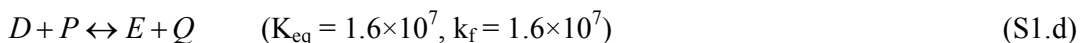
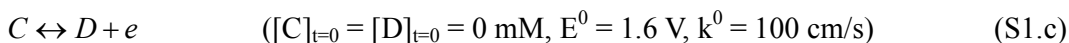
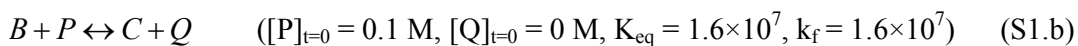
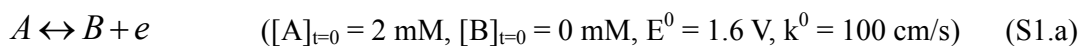


Figure S8. (a) Cyclic voltammogram and (b) chronoamperograms of FTO ( $0.0314 \text{ cm}^2$ ) in pH 6.8 phosphate buffer ( $0.1 \text{ M HPO}_4^{2-}/0.1 \text{ M H}_2\text{PO}_4^-$ ) solution containing  $2 \text{ mM Ni}^{2+}$  (black solid line,  $20 \text{ mV/s}$ ) in comparison with simulated curves of (i) reversible electrochemical one-electron transfer reaction (red solid line in (a), CHI CV simulation (Ver. 14.08) was used with the parameters listed inside figure) and (ii) diffusion-limited current of one-electron transfer reaction (black dot line in (b)). The diffusion coefficient used in the simulation was  $7.59 \times 10^{-6} \text{ cm}^2/\text{s}$ , which is for  $\text{HPO}_4^{2-}$  ([1] "Ionic conductivity and diffusion at infinite dilution", In CRC Handbook of Chemistry and Physics, Lide, D. R. Ed.; CRC Press, Boca Raton, FL, 2005.)

## 9. Numerical Simulation of Catalytic Reaction of Ni<sup>2+</sup> ion in PB solution

The numerical simulation was carried out using CHI CV simulation (Ver. 14.08, CH Instruments, Inc., Austin, TX). For the simulation, the scheme of catalytic reaction (6.a ~ 6.f) was simplified into two electron transfer reactions which are followed by the protonation of HPO<sub>4</sub><sup>2-</sup> (P → Q), respectively, and the step for the regeneration of starting reactant.



$$(D_A = D_B = D_C = D_D = 6.61 \times 10^{-6} \text{ cm}^2/\text{s}, \text{ electrode area} = 0.0314 \text{ cm}^2)$$

Other steps such as the formation of surface species, incorporation of phosphate ion, the change in the crystal structure were discarded for convenience in the simulation. In addition, (S1.a) and (S1.c) were treated as reversible electron transfer (the rate constant,  $k_s = 100$  [cm/s]) though they have obvious irreversible characteristics. The equilibrium constant of reaction (S1.b) and (S1.d) were  $1.6 \times 10^7$  which is the value from (5.g).

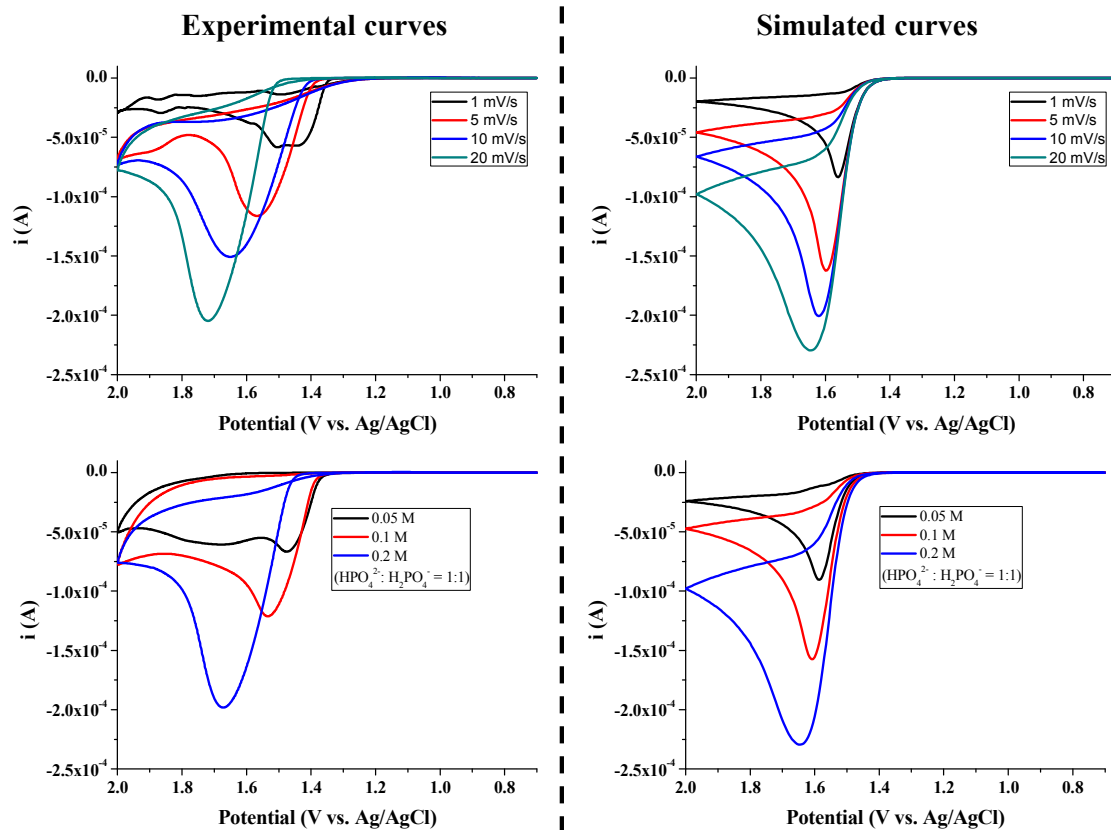


Figure S9. Measured (left) and simulated (right) cyclic voltammograms of catalytic reaction by  $\text{Ni}^{2+}$  for water oxidation with various scan rate and phosphate concentration. The numerical simulation was performed with CHI CV simulation.

10. Photoresponses of  $\text{BiVO}_4$  with  $\text{Ni}^{2+}$  for the oxidation of sulfite and water

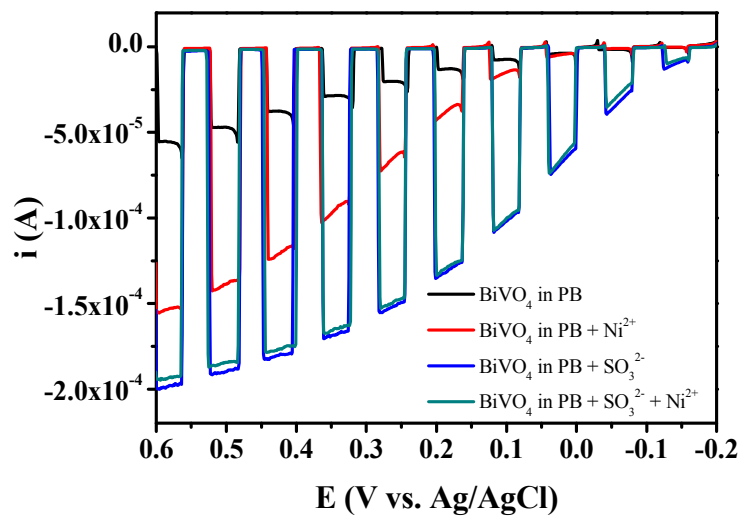


Figure S10. Linear sweep voltammograms (scan rate: 20 mV/s) of  $\text{BiVO}_4$  ( $0.27 \text{ cm}^2$ ) in pH 6.8 phosphate buffer ( $\text{HPO}_4^{2-}$ :  $\text{H}_2\text{PO}_4^-$  =1:1) aqueous solution containing  $\text{Ni}^{2+}$ , with chopped UV-visible light irradiation (full xenon lamp,  $100 \text{ mW/cm}^2$ ),

11. IPCE for the photoelectrochemical water oxidation on BiVO<sub>4</sub> with Ni<sup>2+</sup>

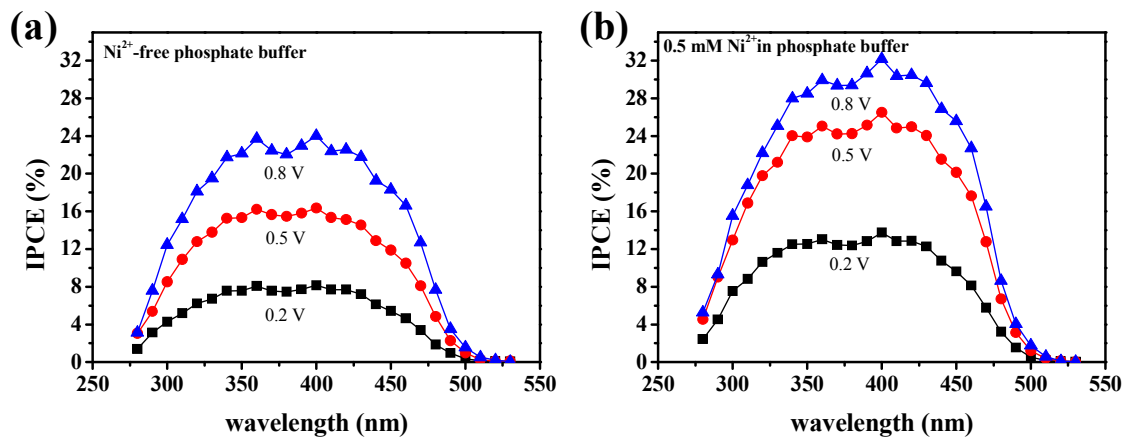


Figure S11. IPCE plots of BiVO<sub>4</sub> photoelectrodes. The photocurrent measured in pH 6.8 phosphate buffer (HPO<sub>4</sub><sup>2-</sup>: H<sub>2</sub>PO<sub>4</sub><sup>-</sup> = 1:1) aqueous solution (a) in the absence of Ni<sup>2+</sup> and (b) in the presence of 0.5 mM Ni<sup>2+</sup>. The light intensity and wavelength were controlled by monochromator and silicon photodetector.

12. CVs of FTO in PB solution containing  $\text{Ni}^{2+}$  in comparison with  $\text{Co}^{2+}$

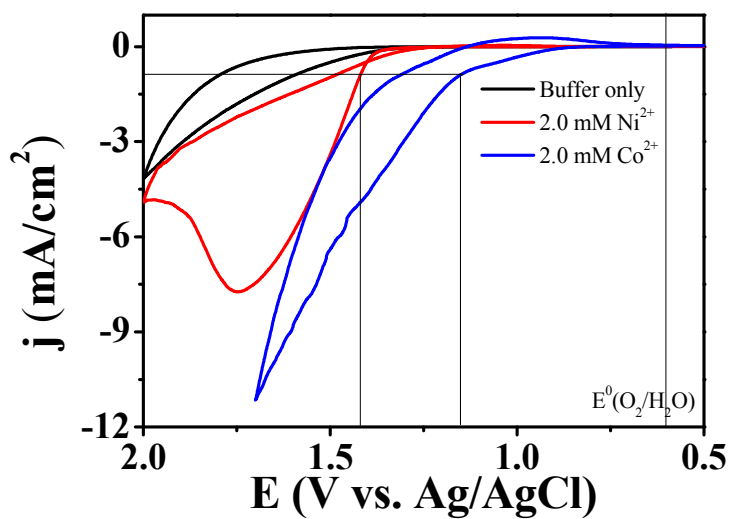


Figure S12. Cyclic voltammogram of FTO (0.0314 cm<sup>2</sup>) in pH 6.8 phosphate buffer ( $\text{HPO}_4^{2-}$ :  $\text{H}_2\text{PO}_4^-$  =1:1) solution containing  $\text{Ni}^{2+}$  or  $\text{Co}^{2+}$  (scan rate: 20 mV/s).



### 13. Rough estimation of turnover frequency of Ni<sup>2+</sup>-WOC

Since Ni<sup>2+</sup>-based heterogeneous catalyst in this study is being deposited and dissociated at each turnover, it is almost impossible to calculate the turnover frequency. Nevertheless, the rough estimation of turnover frequency of Ni<sup>2+</sup>-WOC was attempted as follows;

At 100 s, the current of water oxidation (Fig. S7b) and the amount of Ni(OH)<sub>3</sub> (Fig. 5c) approximately reached the steady-state. The amount of Ni<sup>2+</sup> which has been involved in the water oxidation reaction is equal to that being deposited or being regenerated (per 1 s), and it would be similar in scale to that of the collected charge. Therefore, the turnover frequency was roughly calculated as follows;

Potential	i (t=100 s)	Q <sub>t=100</sub>	TOF (i/4Q <sub>t=100</sub> )
1.5 V ( $\eta = 0.9$ V)	$7.07 \times 10^{-5}$ A	$4.63 \times 10^{-5}$ C	0.382
1.7 V ( $\eta = 1.1$ V)	$7.89 \times 10^{-5}$ A	$2.19 \times 10^{-5}$ C	0.914